Catalysis Letters Vol. 102, Nos. 1–2, July 2005 (© 2005)
DOI: 10.1007/s10562-005-5200-z

X-ray induced surface modification of aluminovanadate oxide

S.P. Chenakin[a], R. Prada Silvy[b], and N. Kruse[a,*]

[a]*Université Libre de Bruxelles (ULB), Chimie–Physique des Matériaux, CP243, Campus Plaine, B-1050 Bruxelles, Belgium*
[b]*Université Catholique de Louvain, Croix du Sud 2, Boite 17, 1348 Louvain-la-Neuve, Belgium*

Received 20 November 2004; accepted 15 February 2005

Aluminovanadate oxide, “V–Al–O”, has been studied by X-ray photoelectron spectroscopy (XPS) with the emphasis to reveal chemical modifications as a function of the X-irradiation time. Considerable damage was found for V–Al–O and less so for vanadium pentoxide, V_2O_5, and sapphire, α-Al_2O_3, both serving as reference samples. Modifications in V–Al–O were seen even at low radiation doses. Absolute and relative shifts in binding energies along with changes of peak intensities and widths demonstrate that an appreciable amount of V^{5+} is reduced to lower oxidation states. X-ray induced chemical modifications extend at least to the depth sampled by the V3p electrons. It is suggested that the damage is caused by electron-hole pair generation and Auger decay. Al–O–H in V–Al–O is also affected by X-rays. This causes O_2 and water desorption as followed by mass spectrometry of the residual gas.

KEY WORDS: X-ray induced damage; XPS; aluminovanadate oxide; V_2O_5.

1. Introduction

X-ray photoelectron spectroscopy (XPS) is being widely used to determine the surface chemical composition of materials. In studies with metal oxides, for example, it may provide valuable information on oxidation states. Using mixed oxides XPS may help identifying chemical building blocks provided charging is under control. X-ray induced sample damage may also occur and has been observed early on. Way back to the seventies molybdenum trioxide, MoO_3, was reported to suffer reduction to MoO_x $(2 < x < 3)$ during prolonged exposure to X-rays [1]. A systematic study of Al $K\alpha$ X-ray-induced surface compositional changes of CeO_2 was carried out by Paparazzo *et al.* [2,3]. The authors found evidence for the occurrence of a reduction process $Ce^{4+} \rightarrow Ce^{3+}$ in the near-surface region and demonstrated that some of the XPS features usually referred to as excited electronic states were, in fact, X-ray induced. In a subsequent XPS study of sintered and un-sintered pellets of CeO_2 radiation-induced formation of sub-stoichiometric oxides was reported [4,5].

Vanadium pentoxide has been demonstrated to be very sensitive to electron irradiation. The +5 oxidation state in V_2O_5 may be reduced even by low-energy electron beams, so that electron spectroscopy should be used deliberately if accurate data are required [6–8]. Surface modifications of V_2O_5 due to X-rays were also reported [8,9]. Both single crystal and polycrystalline V_2O_5 containing small amounts of cadmium at the surface were found to suffer metal reduction by Al $K\alpha$ radiation [10]. Radiation effects in mixed oxides may become rather involved though.

The aim of the present work is to demonstrate that X-rays induce modifications in aluminovanadate oxide (“V–Al–O”). Quantification will be provided in terms of shifts in the binding energy (BE) and full width at half-maximum (FWHM) as a function of the time-of-exposure to Mg $K\alpha$ radiation. Comparison will be made to radiation effects of reference oxides, V_2O_5 and α-Al_2O_3. The high sensitivity of V–Al–O to X-rays was already noted in our previous work [11]. This is different from conclusions reached in studies [12] with nitrified aluminovanadate oxides where neither Al $K\alpha$ radiation nor 10 eV electrons (of a flood gun) caused a visible influence on the spectra during several hours of data acquisition.

2. Experimental

Aluminovanadate oxide was synthesized by co-precipitation from an aqueous solution of aluminium nitrate, $Al(NO_3)_3{\cdot}9H_2O$, and ammonium metavanadate, NH_4VO_3, with a ratio of V/Al = 0.25 (%) at pH = 7.5 adjusted by addition of NH_4OH. For details see reference [11]. The precipitate was filtered, washed several times with hot water and dried at 120 °C overnight, yielding finally a powder with an average particle size of about 230 μm.

V–Al–O samples for XPS analysis were prepared as follows. The powder was either impregnated by iso-propanol (p.A. purity) and subsequently sedimented on a stainless steel backing or compacted uniformly over an indium foil previously fixed on the sample holder to

---

* To whom correspondence should be addressed.
E-mail: nkruse@ulb.ac.be

1011-372X/05/0700–0039/0

form a dense layer ~ 0.1 mm thick. Despite insignificant differences in the results the latter method was preferred for reasons of convenience and reliability (the higher density of the compacted sample caused higher signal intensities and ensured more homogeneous surface charging). V_2O_5 powder (99.6%, Janssen Chimique) and sapphire wafer (α-Al_2O_3) were used as reference samples.

Experiments were performed in a combined XPS/ToF-SIMS instrument with a base pressure of 1.2×10^{-9} mbar. The set-up will be described in detail elsewhere. In brief, non-monochromatic Mg $K\alpha$ radiation was used at a power of 15 kV × 10 mA. The samples were outgassed during 160 h in a preparation chamber at a base pressure of 5×10^{-10} mbar. The incidence angle of the photons was 19° with respect to the sample surface normal. The illuminated area was about 0.4 cm^2. Photoelectron spectra were acquired as a function of irradiation time using a hemispherical analyzer (at a take-off angle of 50°) in the constant-pass-energy mode at $E_p = 50$ eV. The overall resolution of the spectrometer in this operating mode was 0.96 eV measured as FWHM of the $Ag3d_{5/2}$ line. The spectrometer was calibrated against $E_b(Au4f_{7/2}) = 84.0$ eV and $E_b(Cu2p_{3/2}) = 932.4$ eV. The Al *KLL* Auger spectra were recorded using the energetic region of the Bremsstrahlung. If necessary, binding energies were corrected for surface charging using adventitious carbon C1s at 285 eV as reference. Samples were subjected to X-rays during up to 3 h at room temperature. The data acquisition started immediately after the sample was moved under the running X-ray source. The first acquired spectrum was defined as that corresponding to a virgin surface and "zero-time" exposure. Temperatures at the V–Al–O sample surface were measured with a Ni–NiCr thermocouple pressed into the powder layer. Gas evolution during X-ray analysis was monitored by a quadrupole mass spectrometer (Hiden Analytical).

After background subtraction, the Al2p and the O1s–V2p core-level spectra were fitted by mixed Gaussian–Lotentzian lines with due account of the X-ray satellite. The surface composition was evaluated from peak areas. Relative sensitivity factors were determined from the reference compounds V_2O_5 and Al_2O_3: O(1s):V($2p_{3/2}$):Al(2p) = 1:1.91:0.25. XPS measurements as a function of radiation dose were performed three times for each sample and the results were found to be reproducible.

3. Results

Figure 1a shows the O1s–V2p spectral region (scan time 75 s) of the compacted V–Al–O catalyst in the initial state at "zero" exposure (top) and after X-ray irradiation for 150 min (bottom). The BE scale has been corrected for charging effects. Broad peaks in both spectra centered around ~ 531, 523 and 517 eV correspond to O1s, $V3p_{1/2}$ and $V3p_{3/2}$ transitions, respectively. The Al2p peak (not shown in figure 1a) was located at 74.1 eV. The O1s–V2p spectrum of virgin V_2O_5 (scan time 72 s) and the O1s line of Al_2O_3 (scan time 38 s) in the initial state are shown in figure 1b for comparison.

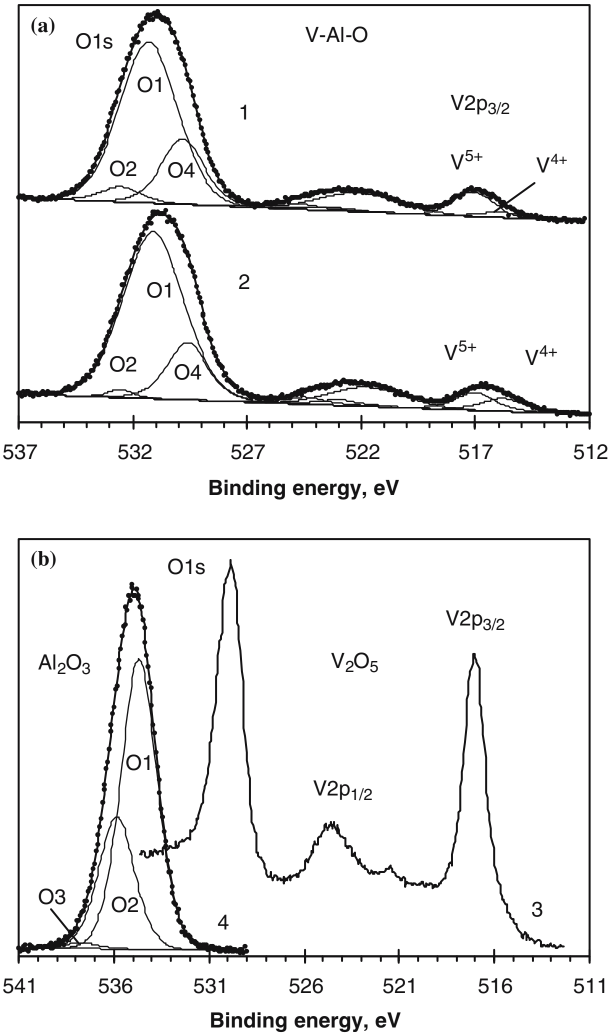

Figure 1. (a) O1s–V2p spectral region of the V–Al–O catalyst in the initial state (1) and after X-ray irradiation for 150 min (2). The binding energy scale is charge-corrected. The results of the spectra deconvolution are also shown, with the components O1, O2, O4 in the O1s envelope representing Al–O–Al, Al–O–H and V–O–V oxygen environments, respectively. (b) O1s–V2p region of virgin V_2O_5 (3) and O1s spectrum (no BE correction for charging effects is applied) of α-Al_2O_3 in the initial state (4). The components O1, O2, O3 in the O1s envelope of Al_2O_3 represent Al–O–Al, Al–O–H and H–O–H bonds, respectively.

In figure 2 the evolution with time of FWHM and BE of the main peaks is demonstrated for the V–Al–O catalyst. It is seen that the O1s and Al2p peaks slightly broaden and shift in position to somewhat higher BE's. By contrast, the $V2p_{3/2}$ peak suffers substantial broadening along with a shift to lower BE's.

The results of figure 2 suggest that Mg $K\alpha$ radiation causes time-dependent structural and compositional

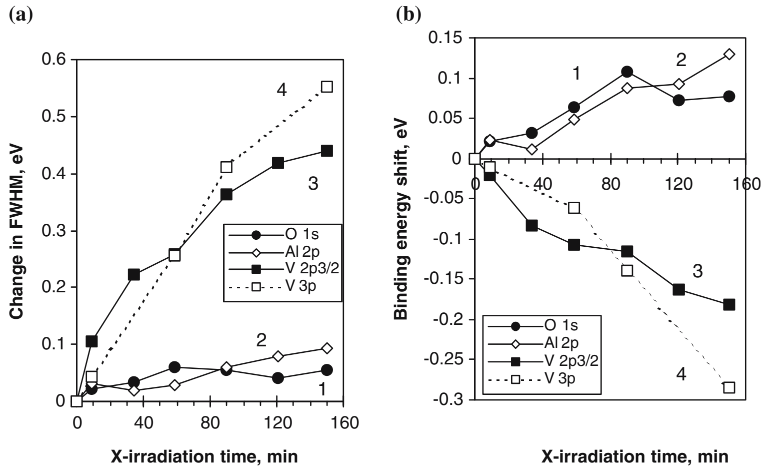

Figure 2. Change in FWHM (a) and binding energy shift (b) of the O1s (1), Al2p (2), V2p$_{3/2}$ (3), and V3p (4) peaks as a function of the time of exposure of the V–Al–O catalyst to Mg *K*α X-ray radiation with reference to the sample in the initial state.

changes in the V–Al–O catalyst. In order to allow for a more quantitative assessment of the observations, we now consider the reference spectra of V_2O_5 and Al_2O_3 at "zero" exposure. Turning to the O1s–V2p spectral region of V_2O_5 first, we find that the O1s and V2p$_{3/2}$ transitions occur at 529.8 and 517 eV, respectively (along with a broad V2p$_{1/2}$ feature around 524.5 eV). Peak locations and widths (FWHM 1.6 eV for O1s and 1.4 eV for V2p$_{3/2}$) are in good agreement with those of Mendialdua *et al.* [10]. The V2p$_{3/2}$ feature for the virgin V–Al–O catalyst (FWHM 2.3 eV) is significantly broader than that for V_2O_5 under the same conditions indicating the occurrence of vanadium oxidation states less than +5 in the former (a more quantitative estimation provides a value of +4.8 on average).

Not only the V2p$_{3/2}$ but also the O1s peak is much broader in V–Al–O (FWHM 3.6 eV) than in V_2O_5. This indicates a larger variety in the chemical environments of the oxygen atom in V–Al–O. A more detailed assessment becomes possible if we also consider the O1s peak width in Al_2O_3 (FWHM 2.68 eV), which is intermediate between V_2O_5 and V–Al–O. The asymmetrical O1s spectrum of virgin Al_2O_3 can be deconvoluted as demonstrated in figure 1b, assuming Al–O–Al (O1), Al–O–H (O2) and H–O–H (O3) local chemical structures to arise as a result of hydroxylation of the surface. Obviously, only V–O–V groups (O4) contribute to the respective spectrum of V_2O_5. Accordingly, three most abundant environments for oxygen, Al–O–Al, V–O–V and Al–O–H, can be assumed to be present in V–Al–O. Deconvolution the O1s–V2p region with these components shows (figure 1a) that the V–Al–O catalyst in the initial state contains V–O–V and Al–O–Al bonds at a ratio O4/O1 ~ 0.3 which is close to the bulk composition (atomic ratio V/Al = 0.25). The modified oxygen Auger parameter $\alpha'(O) = KE(OKLL) + BE(O1s) = 1039.3$ eV in V–Al–O is seen to be noticeably different from that of V_2O_5 (1043.2 eV) but close to $\alpha'(O)$ of Al_2O_3 (1039.0 eV) indicating Al–O–Al environments to dominate.

For both reference samples, V_2O_5 and Al_2O_3, the FWHM and BE time dependencies of the V2p$_{3/2}$, O1s and Al2p transitions have likewise been measured. Although the detailed results will be published elsewhere we mention that the changes in the FWHM and BE of the V2p$_{3/2}$ peak for V_2O_5 are considerably smaller (by roughly a factor of two after 150 min of X-irradiation) than those for V–Al–O (figure 2). On the other hand, the changes in FWHM and BE of the Al2p peak for Al_2O_3 are relatively weak (for example, ΔBE does not exceed +0.15 eV) and comparable to those for V–Al–O. As to the O1s peak in V_2O_5, neither the FWHM nor the BE change noticeably with time. This is quite different from the α-Al_2O_3 reference where both FWHM and BE of the O1s transition decrease by amounts of ~ 0.15–0.2 eV and ~ 0.1 eV, respectively, after 150 min of exposure to Mg *K*α. Concurrently, a substantial loss of oxygen occurs from the surface under irradiation as a result of desorption of water in an associative mechanism involving mainly surface hydroxyl/oxo-hydroxyl.

Summarizing the observations made in figures 1 and 2 it is clear that Mg *K*α radiation causes strong compositional changes in V–Al–O. These changes are stronger than in Al_2O_3 and V_2O_5 references (as will be shown elsewhere in detail). With growing X-ray exposure we find the fraction of V^{4+} in the deconvoluted V2p$_{3/2}$ peak to rise and attain about 45% at maximum exposure (figure 1a, bottom). At the same time the concentration of V–O–V bonds decreases (the ratio O4/O1 drops to ~ 0.23) and the fraction of Al–O–H bonds is reduced from 5 to 1.5%.

The behavior of the low-BE peaks, O2s and V3p, in V–Al–O under X-ray exposure may allow for an estimation of the sampling depth. While the O2s peak (not shown) experiences minor changes, the V3p peak clearly displays a noticeable broadening and a shift to lower

BE's with time of exposure to Mg *K*α (figure 2, curves 4). In view of the difference in kinetic energy for the V2p$_{3/2}$ and V3p electrons (737 and 1212 eV, respectively) it must be inferred that X-rays induce chemical modifications at least to the depth sampled by the V3p electrons. We have evaluated the sampling depth (which contributes to 95% of the total peak intensity and equals ~ 3 times the inelastic mean free path [13]) to be 11.8...13.2 nm and 15.2...16.8 nm for the V2p and V3p electrons, respectively.

The initial surface composition of the V–Al–O catalyst has been evaluated to be 4.7V–26.1Al–69.2O (%). During exposure to X-radiation the oxygen concentration decreases and the surface becomes slightly enriched in Al (figure 3). The strongest change in the surface concentration obviously occurs during the first 50–60 min of the measurements.

We have also measured the catalyst temperature during X-ray exposure. Accordingly, a gradual increase by 10 K is seen; after 80–90 min of irradiation the final temperature of V–Al–O reaches ~ 309 K. At the same time, a gradual desorption of water occurs as revealed by mass spectrometric monitoring of the residual atmosphere. As a result of the exposure to Mg *K*α, the color of the sample surface turns brownish from green–yellow initially.

4. Discussion

The degradation of V–Al–O catalysts under X-radiation can be depictured as follows. According to studies reported elsewhere [11], the structure of the catalyst at pH = 7.5 is given in the form of a polymer network of linked tetrahedral $[VO_x]_n^{n-}$ units supported by amorphous aluminium hydroxide. X-rays affect preferentially the vanadium oxide subsystem and break V–O–V bonds whose abundance decreases (figure 1a). Accumulating damage brings about reduction of V^{5+} ions, the amount of the initially available V^{4+} species grows by a factor of more than 2 and the average vanadium oxidation state in the catalyst reaches +4.55. The dark color of the irradiated surface also indicates abundant formation of V^{4+} species because all vanadium oxides with an oxidation state lower than 5+ are black. As a result, the V 2p$_{3/2}$ peak appreciably broadens and shifts to lower BE's (figure 2), and the final V 2p$_{3/2}$ BE corresponds to that reported for V_4O_9 [10]. The in-depth X-ray induced damage is estimated as being at least 16 nm, which is the sampling depth of the V 3p electrons in V–Al–O. Previous studies of the in-depth damage of CeO_2 by X-rays have been much under debate [4,5].

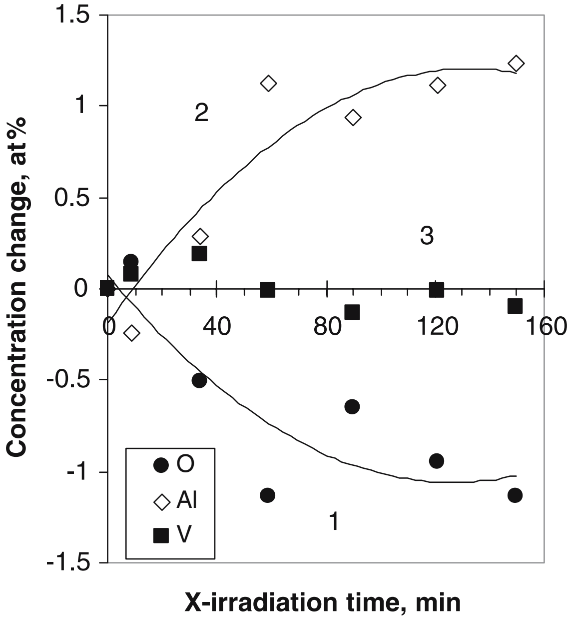

Figure 3. Variation of the surface concentration of oxygen (1), aluminium (2) and vanadium (3) in V–Al–O during X-irradiation with reference to a virgin sample.

X-rays also cause breaking of Al–O–H bonds in V–Al–O (figure 1a). This leads to water formation and desorption as seen by residual gas analysis. Part of the total loss of surface oxygen (figure 3) is certainly due to the rupture of surface hydroxyl. The changes under the influence of X-rays in both FWHM and BE of the Al 2p peak, which are similar to those in hydroxide-terminated α-Al_2O_3, provide further corroborating evidence for this process.

The present communication has demonstrated considerable X-ray induced modifications in V–Al–O. Although a cross-comparison with V_2O_5 and Al_2O_3 will be presented elsewhere it is worth noting here that the damage decreases in order of mention. Some reduction to V^{4+} was observed in V_2O_5, however, the V–Al–O catalyst proved to be most susceptible to X-radiation. The different reducibility of vanadium ions in V–Al–O and in V_2O_5 indicates structural effects to be of importance: while V is octahedrally coordinated in V_2O_5 and thus relatively stable with respect to reduction, it is tetrahedrally coordinated in V–Al–O. Quite similarly, oxygen atoms in tetrahedral $[VO_x]_n^{n-}$ units linked to form a polymer network may be supposed to be less strongly bound than in V_2O_5.

We now proceed to a physical interpretation of our observations. A concept of intense local heating of the surface by X-rays as a main damaging factor was employed in references [2,3] to explain the reduction of ceria. The present experiments show that thermally induced processes alone cannot explain the results since the temperature at the surface of V–Al–O after 3 h of irradiation did not exceed 36 °C. Apparently, other mechanisms involving electronic rearrangements must be considered [3,4].

There are two main mechanisms that can explain radiation-induced damage in oxides: electron-hole pair generation and Auger decay [14]. Energetic photo- and secondary electrons propagating in a solid can excite valence band electrons promoting their transition to the conduction band. This leads to the generation of electron-hole pairs. From the physical point of view, a hole in the valence band of an insulator corresponds to a bond being broken between two atoms (i.e. between metal and oxygen in oxides). Electrons resulting from electron-hole pair generation and escaping into the vacuum leave behind a positively charged surface. The arising electric field reduces the probability of the electron-hole recombination. This factor may also contribute to a higher degree of damage in insulating V–Al–O than in V_2O_5. In oxides, Auger decay following photoionisation of the O 1s level creates two holes in the valence band, while the Auger cascade following ionization of the metal 1s (Al) or 2s level (V) may leave multiple holes in the same valence band. X-ray induced V $L_3M_{23}M_{45}$ Auger spectra of V–Al–O show that the O2p and V3d valence electrons are involved in the decay. Multiple hole states in the valence band cause breaking of bonds between V and O (or between Al and OH) and thus lead to reduction of V ions with subsequent desorption of oxygen as a neutral molecule. Both the electron-hole pair generation and the Auger decay are processes that occur up to the penetration depth of X-rays [14], so that the radiation-induced reduction of V ions could be observed within the sampling depth of the V 3p electrons in our studies.

5. Conclusions

Aluminovanadate oxide, V–Al–O, suffers structural and chemical damage while interacting with X-rays. A decrease in the oxygen surface concentration has been found along with an appreciable reduction of V^{5+}–V^{4+} (the fraction of the V^{4+} species initially present in the oxide increases from $\sim$ 20 to 45%) and a decomposition of aluminium hydroxide. Thermal effects cannot explain the damage alone since the surface temperature during irradiation increases only slightly. The damage is believed to be caused by electron-hole pair generation and Auger decay and extends to a significant depth. In view of the high susceptibility of V–Al–O to X-rays short-time XPS analysis is mandatory to provide data free of artifacts.

Acknowledgments

The authors thank the Direction Générale des Technologies, de la Recherche et de l'Énergie de la Région Wallonne (GREDECAT) for the financial support, and N. Blangenois for her help in preparing the catalyst.

References

[1] J. Grimblot and J.P. Bonnelle, Comptes Rendus des Seances Acad. Sci., Ser. C 282 (1976) 399.

[2] E. Paparazzo, Surf. Sci. 234 (1990) L253.

[3] E. Paparazzo, G.M. Ingo and N. Zacchetti, J. Vac. Sci. Technol. A 9 (1991) 1416.

[4] M.V. Rama Rao and T. Shripathi, J. Electron Spectrosc. Relat. Phenom. 87 (1997) 121.

[5] E. Paparazzo and G.M. Ingo, J. Electron Spectrosc. Relat. Phenom. 95 (1998) 301.

[6] E. Suoninen, E. Minni and I.M. Curelaru, J. Microscopie Spectrosc. Electroniques 6 (1981) 1.

[7] H.G. Tompkins, I.M. Curelaru, K.S. Din and E. Suoninen, Appl. Surf. Sci. 21 (1985) 280.

[8] Z. Zhang and V.E. Henrich, Surf. Sci. 321 (1994) 133.

[9] S. Suzer, Appl. Spectroscopy 54 (2000) 1716.

[10] J. Mendialdua, R. Casanova and Y. Barbaux, J. Electron Spectrosc. Relat. Phenom. 71 (1995) 249.

[11] N. Blangenois, M. Florea, P. Grange, R. Prada Silvy, S.P. Chenakin, J.-M. Bastin, N. Kruse, B.P. Barbero and L. Cadús, Appl. Catal. A 263 (2004) 163.

[12] H. Wiame, L. Bois, P. Lharidon, Y. Laurent and P. Grange, Sol. State Ionics 101–103 (1997) 755.

[13] D. Briggs(ed.), *Handbook of X-ray and Ultraviolet Photoelectron Spectroscopy* (Heyden, London, 1977) p.158.

[14] J. Cazaux, J. Electron Spectrosc. Relat. Phenom. 105 (1999) 155.